[CANCER RESEARCH 59, 3565–3569, August 1, 1999]

Advances in Brief

Caspase Inhibition in Camptothecin-treated U-937 Cells Is Coupled with a Shift from Apoptosis to Transient G_1 Arrest Followed by Necrotic Cell Death[1]

Alain-Théophile Sané and Richard Bertrand[2]

Research Centre of the University of Montreal, Notre-Dame Hospital, Montreal Cancer Institute, Montreal, Quebec, H2L 4M1 Canada

Abstract

Leukemia U-937 cells rapidly undergo characteristic morphological changes, caspase activation, and DNA fragmentation typical of apoptosis on treatment with the DNA topoisomerase I inhibitor camptothecin (CPT). In a previous report (Sané, A. T., and Bertrand, R., Cancer Res., *58:* 3066–3072, 1998), we showed that, after CPT treatment, caspase inhibition by the tripeptide derivative benzyloxycarbonyl-Val-Ala-Asp(Ome)-fluoromethyl ketone (zVAD-fmk) blocked apoptosis and slowed passage of the cells through S-G_2 and caused a transient accumulation of these cells at the G_1 phase of the cell cycle. Accumulation of these cells at G_1 is not associated with major changes in expression level of cyclin-dependent kinase (cdk)2, cdk4, and cdk6; cyclin D1 and cyclin E; or p16, p21, p27, and p57 after CPT treatment. Furthermore, cdk2, cdk4, and cdk6 kinase activities remain unaffected after CPT treatment. These results indicate that the G_1 arrest of these cells does not correlate with a classical driven cell cycle checkpoint but with the known effect of CPT in mediating inhibition of DNA replication and RNA transcription after stabilization of topoisomerase I-linked DNA strand breaks. However, persistent caspase inhibition after CPT treatment also results in cells falling into necrosis after the transient G_1 arrest. These results indicate that the enforced inhibition of caspase activities does not confer a survival advantage upon CPT-treated cells but is coupled with a shift from apoptosis to transient G_1 arrest followed by massive necrosis.

Introduction

top 1[3] and top 2 inhibitors are cytotoxic anticancer drugs that stabilize a transient intermediate of topoisomerase reactions in which enzymes are linked to the 3′ (top 1) or 5′ (top 2) terminus of a DNA duplex producing DNA single- or double-strand breaks. These topoisomerase-linked DNA strand breaks are reversible prelethal lesions that inhibit DNA metabolism such as replication and transcription (1, 2). Although reversible, topoisomerase-linked DNA strand breaks signal G_1 or G_2 cell cycle checkpoints in some cells but rapidly induce apoptosis in others, with the activation of aspartic acid-specific cysteine proteases known as caspases (3–12). Caspase activities drive proteolysis of specific homoeostatic and structural proteins that results in an irreversible commitment of cells to undergo apoptosis (13, 14). Many studies strongly suggest now that the mitochondrial pathway of caspase activation plays the central role in cell death induced by genotoxic drugs (15). Cells deficient in Apaf-1 or caspase-9 are protected from apoptosis induced by anticancer drugs (16, 17). The complex formation between cytochrome *c*, Apaf-1, and caspase 9 zymogen leads to the cleavage and activation of caspase 9 that in turn activates directly the effector caspase-3 and -7 (16, 17). Caspase-3 activity accounts for the proteolysis of several substrates including DFF/mICAD, the proteolysis of which releases DFF40/CPAN/mCAD, which then enters the nucleus and initiates chromosomal DNA fragmentation (18–20). Caspase activation is also associated with morphological changes typical of apoptosis and characterized by cytoplasmic shrinkage, membrane blebbing, chromatin condensation, and extensive DNA breakage (21).

In previous studies (12), we showed that the inhibition of caspase activities by zVAD-fmk after CPT treatment, caused transient accumulation of the cells at the G_1 phase of the cell cycle. In this study, we investigated the molecular determinants of the accumulation of these cells at G_1 and their fate after long-term, enforced inhibition of caspase activities after CPT treatment. We show that specific cyclins, cdks, and cdk inhibitors, the expression and activity of which are associated with G_1-S transition, remain unaltered in caspase-inhibited CPT-treated cells. These observations suggest that the accumulation of the cells at the G_1 boundary is associated with the effect of CPT in mediating the inhibition of DNA replication and RNA transcription after stabilization of top 1-linked DNA strand breaks. We show also that the G_1 arrest was only transient and followed by massive necrosis in the caspase-inhibited CPT-treated U-937 cells. Thus, inhibition of caspase activities in CPT-treated cells does not confer a survival advantage for CPT-treated cells but is coupled with a shift from apoptosis to transient G_1 arrest and massive necrosis.

Materials and Methods

Chemicals. CPT was purchased from Sigma Chemical Co. (St. Louis, MO). The fluorogenic peptide derivative Ac-Asp-Glu-Val-Asp-amino-4-methylcoumarin was purchased from Bachem Bioscience Inc. (King of Prussia, PA). The caspase inhibitor tripeptide derivative zVAD-fmk was purchased from Enzyme Systems Products (Livermore, CA). Methyl-[^{3}H]-thymidine (78 Ci/mmol) and [γ-^{32}P]ATP (>4000 Ci/mmol) were purchased from ICN BioMedicals (Costa Mesa, CA). All of the other chemicals were of reagent grade and purchased either from Sigma Chemical Co. and ICN BioMedicals or from other local sources.

Cell Culture and Drug Treatments. The human U-937 cell line was obtained from the American Type Culture Collection (Manassas, VA). Cells were grown in suspension culture at 37°C under 5% CO_2 in a humidified atmosphere in RPMI 1640 supplemented with 10% heat-inactivated fetal bovine serum, 2 mM glutamine, 100 units/ml penicillin and 100 μg/ml streptomycin. Cell culture products were obtained from Life Technologies, Inc. (Grand Island, NY). Exponentially growing cells were used throughout all of the experiments at a density of 5×10^5 cells/ml. Cells were treated with CPT at 1.0 μM in the absence or presence of 300 μM zVAD-fmk. After a 30-min incubation at 37°C, cells were pelleted by centrifugation, washed, and resuspended in fresh medium with or without zVAD-fmk.

Analysis of DNA Content by Flow Cytometry. Cells were centrifuged at $1000 \times g$ for 2 min and washed in ice-cold PBS. Cell pellets were fixed in 70% ethanol for 2 h at 4°C. After incubation, cells were pelleted by centrifugation and resuspended in a solution of 70% ethanol containing 150 μg/ml RNase A and

Received 3/15/99; accepted 6/21/99.

The costs of publication of this article were defrayed in part by the payment of page charges. This article must therefore be hereby marked *advertisement* in accordance with 18 U.S.C. Section 1734 solely to indicate this fact.

[1] This work was supported by the Medical Research Council of Canada (MT-15019). R. B. obtained a scholarship from the Medical Research Council of Canada and the Research Cancer Society Inc. A. T. S. was supported by studentships obtained from the Faculté des Etudes Supérieures (Université de Montréal).

[2] To whom requests for reprints should be addressed, at Research Centre of the University of Montreal, Notre-Dame Hospital, Montreal Cancer Institute (Room Y-5634), 1560 Sherbrooke Street East, Montreal, Quebec, H2L 4M1 Canada. Phone: (514) 281-6000; Fax: (514) 896-4689; E-mail: bertranr@ere.umontreal.ca.

[3] The abbreviations used are: CPT, 20-S-camptothecin lactone; top 1, DNA topoisomerase 1; top 2, DNA topoisomerase II; cdk, cyclin-dependent kinase; zVAD-fmk, benzyloxycarbonyl-Val-Ala-Asp(Ome)-fluoromethyl ketone; DEVDase, Asp-Glu-Val-Asp protease activities; TAFE, transverse alternating pulsed field electrophoresis; PMSF, phenylmethylsulfonyl fluoride.

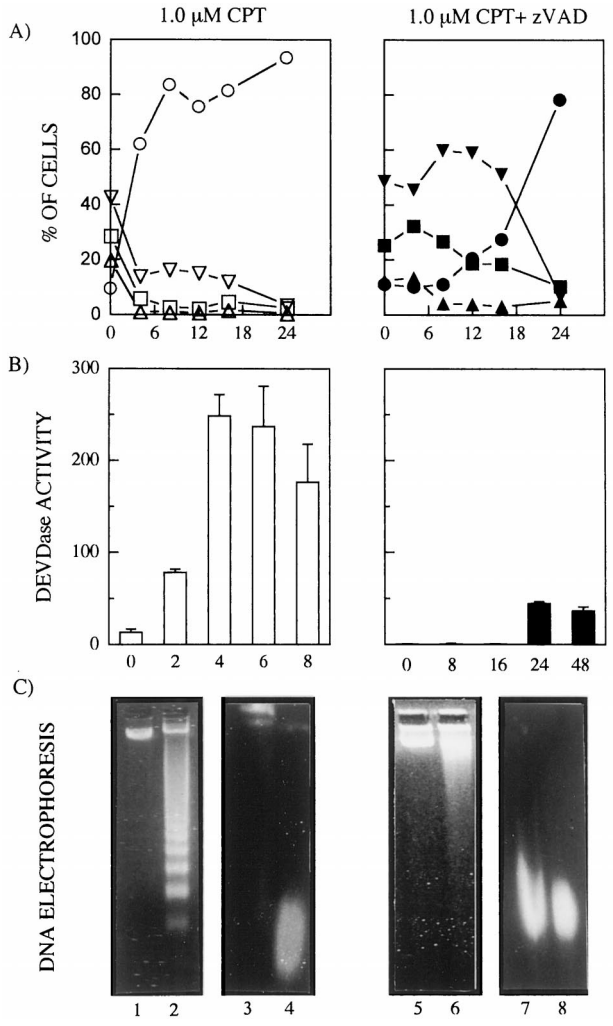

Fig. 1. The effects of caspase inhibition in CPT-treated U-937 cells. *A*, cell cycle progression after CPT treatment in the absence (*left*) and presence (*right*) of zVAD-fmk. At the indicated times (in h) after CPT treatment (*x axis*), cells were processed for flow cytometry analysis. ○ and ●, sub-G_0-G_1; ▽ and ▼, G_0-G_1; □ and ■, S phase; △ and ▲, G_2-M. *Data points*, mean of two independent experiments (less than 10% difference between experiments). *B*, caspase activities after CPT treatment in the absence (*left*) and presence (*right*) of zVAD-fmk. At the indicated times (in h) after CPT treatment (*x axis*), DEVD-AMC hydrolysis was measured by fluorospectrometry. Enzyme activities were measured as initial velocities and expressed as relative intensity/min/mg. *Data points*, means of three independent determinations; *bars*, SE. *C*, DNA fragmentation pattern after CPT treatment in the absence (*left*) and presence (*right*) of zVAD-fmk. DNA fragmentation was analyzed by standard agarose gel electrophoresis (*Lanes 1, 2, 5* and *6*) and TAFE (*Lanes 3, 4, 7*, and *8)*. After electrophoresis, DNA was visualized by ethidium bromide staining. *Lanes 1* and *3*, control U-937 cells; *Lanes 2* and *4*, 4 h after CPT treatment; *Lanes 5* and *7*, 24 h after CPT treatment + zVAD-fmk; *Lanes 6* and *8*, 48 h after CPT treatment + zVAD-fmk.

incubated for 30 min at room temperature. Cells were then pelleted by centrifugation and resuspended in PBS. Propidium iodide (50 μg/ml) was added before cytofluorometry analysis. DNA content and cell cycle distribution were analyzed using a Becton Dickinson FACStar Plus flow cytometer (12).

Determination of DEVDase Activities. Control and drug-treated U-937 cells were pelleted by centrifugation, washed twice in ice-cold PBS, and resuspended in lysis buffer containing 10 mM HEPES (pH 7.4), 80 mM KCl, 20 mM NaCl, 5 mM $MgCl_2$, 5 mM EGTA, 1 mM DTT, 1 mM PMSF, 0.15 units/ml aprotinin, 10% glycerol, and 0.3% NP40, as described previously (22). DEVDase activities were measured by continuous fluorescence monitoring in a dual-luminescence fluorometer (model LS 50B, Perkin-Elmer) using an excitation wavelength of 380 nm and an emission wavelength of 460 nm. Reactions were carried out in cuvettes, and the temperature was maintained at 37°C using a water-jacketed sample compartment. The assay mixture contained 100 mM HEPES (pH 7.4), 20% glycerol, 5 mM DTT, 5 mM EDTA, 100 μM fluorogenic peptide, and 200 μg cytosolic extract. Enzyme activities were measured as initial velocities and expressed as relative intensity/min/mg (12).

Analysis of DNA Fragmentation by Agarose Gel Electrophoresis. To visualize the oligonucleosome-sized DNA fragments cellular DNA was extracted by a salting-out procedure as described previously (5). Electrophoresis was done in 1.6% agarose gel in Tris-acetate buffer (pH 8.0). High molecular weight DNA fragments were analyzed by TAFE using a Beckman Geneline apparatus (Beckman Instruments Inc., Paolo Alto, CA). Agarose blocks containing cells were incubated for 24 h at 42°C in a solution containing 1.0 mg/ml proteinase K, 1% *N*-lauryl-sarcosine, 0.2% sodium deoxycholate, and 100 mM EDTA (pH 8.0). The agarose-embedded DNA was soaked in TE buffer [20 mM Tris-HCl (pH 8.0) and 50 mM EDTA] before electrophoresis on a 1.2% agarose gel. Gels were subjected to a 30-min run at 170 V with a pulse time of 4 s, followed by a 24-h run at 150 V with a pulse time of 60 s. Electrophoresis was done at 18°C in TAFE buffer [10 mM Tris, 5 mM EDTA-free acid, and 0.025% (v/v) glacial acetic acid (12)]. After electrophoresis, DNA was visualized by ethidium bromide staining.

Measurement of Thymidine Incorporation. Control and drug-treated cells (2×10^6 cells) were collected, and cell samples were divided equally in two aliquots for thymidine incorporation assay and protein concentration determination. Rates of thymidine incorporation were measured by 10-min pulse experiments with [^{3}H]thymidine (10 μCi/ml) incorporation as described (23). Nucleotide incorporation was stopped by adding 10 ml of ice-cold PBS, and cells were quickly pelleted by centrifugation. Acid-insoluble nucleotides were precipitated on ice with 10% trichloroacetic acid. Precipitates were dissolved in 0.4 N NaOH, and radioactivity was monitored by scintillation spectrometry. Total protein concentrations were determined using the Bradford assay (Bio-Rad, Hercule CA). The rate of DNA synthesis was expressed as cpm/mg, and data obtained from drug-treated cells were expressed as relative to control cells (23).

Western Blot Analysis. Control and drug-treated cells were collected by centrifugation, washed once with ice-cold PBS, and then homogenized in a lysis buffer containing 5 mM HEPES (pH 7.4), 160 mM KCl, 40 mM NaCl, 10 mM $MgCl_2$, 1.0 mM PMSF, 1.0 mM DTT, 1.0% NP40, and a cocktail of protease inhibitors (Complete, Boehringer-Mannheim) at 4°C for 30 min with gentle agitation. After centrifugation (10,000 × *g* for 10 min), supernatants were collected. Mouse monoclonal antibodies used for Western blot analysis were cdk2 (D-12), cyclin D1 (R-124), and p27 (F-8) from Santa Cruz Biotechnology Inc. (Santa Cruz, CA) and p21 (Ab-1) and p16 (Ab-1) from Oncogene Research Products (Cambridge, MA); rabbit polyclonal antibodies cdk6 (H-230), cdk4 (C-22), cyclin E (M-20), and goat polyclonal antibodies p57 (C-20)-G were from Santa Cruz Biotechnology. Immunoblot analysis was performed accordingly with the horseradish peroxidase-conjugated antimouse, or antirabbit, or antigoat antibodies using Enhanced Chemiluminescence (ECL) Western Blotting Detection reagents (Amersham Life Science).

Kinase Assays. Two × 10^6 control or drug-treated cells were pelleted and washed in ice-cold PBS. Cells were lysed on ice in PBS lysis buffer containing 10 mM sodium orthovanadate, 2 mM PMSF, 1 mg/ml aprotinin, 1% BSA, a cocktail of protease inhibitors (Complete, Boehringer-Mannheim), and 1% NP40 for 30 min. Insoluble material was removed by centrifuging at 3000 rpm for 15 min at 4°C. Supernatant was incubated with 2 μg of goat anti-Cdk2 (M-2), goat anti-Cdk4 (H-22), or goat anti-Cdk6 (C-21; Santa Cruz Biotechnology) and rabbit anti-cdc2/cdk1 (Ab-1) obtained from Calbiochem-Novabiochem Corporation (San Diego, CA). Immune complexes were trapped by protein A/G Plus-Sepharose and pelleted by centrifugation. Pellets were resuspended and incubated for 20 min in 30 μl kinase assay buffer containing 20 mM Tris-HCl (pH 7.5), 1 mM sodium orthovanadate, 10 mM $MgCl_2$, 5 μM ATP, 10 μCi [γ-^{32}P]ATP, and 5 μg of purified histone H1 (Life Technologies, Inc.) as substrate. Reactions were carried out at 37°C for 20 min, stopped by the addition of 5 μl of 3× concentrated electrophoresis Laemeli sample buffer, and boiled for 5 min. Samples were centrifuged, and the soluble fractions were loaded on SDS-PAGE. After electrophoresis, gels were dried and exposed to X-ray film.

Electron Microscopy. Cells were centrifuged at 400 × *g* for 10 min and washed in ice-cold PBS. Cell fixation was performed in 0.1 M Millonig's phosphate buffer [(pH 7.4); 292 milliosmoles] containing 2.5% glutaraldehyde. Staining was performed with 2% uranyl acetate, and dehydration was performed with several ethanol treatments. Sections (500–700 Å) were mounted on copper grids and stained in lead citrate. Samples were examined (JFE Enterprises, Brookville, MD) by transmission electron microscopy using a Ziess Em 10 CA microscope.

Results and Discussion

Effect of Caspase Inhibition by zVAD-fmk in CPT-treated U-937 Cells. Short CPT treatment rapidly triggers apoptosis in U-937 cells (12). Flow cytometry analysis after CPT treatment indicates that cells do not accumulate in a specific phase of the cell cycle but appear rapidly in a sub-G_0-G_1 peak. Approximately 60 and 80% of the cells are localized in the sub-G_0-G_1 peak 4 h and 8 h after CPT treatment, respectively (Fig. 1*A*, *left*). In CPT-treated cells, DEVDase activities—a measure of caspase-3, -7 and -2 activities (24)—are rapidly detected after drug treatment (Fig. 1*B*, *left*). Caspase activities correlate also with the appearance of oligonucleosome-sized and high molecular weight DNA fragmentation visualized by ethidium bromide staining following standard agarose gel electrophoresis and TAFE, respectively (Fig. 1*C*, *left*). We reported previously (12) that the inhibition of caspase activities in CPT-treated cells by zVAD-fmk blocks apoptosis. In the presence of zVAD-fmk, passage through S-G_2 of CPT-treated cells is slowed and approximately 60% of cells accumulate at the G_0-G_1 phase of the cell cycle for at least 16 h (Fig. 1*A*, *right*). Sub-G_0-G_1 cells appear slowly 12 h after CPT-treatment in the presence of zVAD-fmk but increase dramatically between 16 and 24 h posttreatment, with more then 80% of cells in sub-G_0-G_1 peak 24 h after treatment. The increase in sub-G_0-G_1 cell population correlates with the fall of G_0-G_1 cell population (Fig. 1*A*, *right*). No DEVDase activities are detected in CPT-treated cells in the presence of zVAD-fmk when cells accumulate in G_0-G_1. Moreover, when cells appear predominantly in sub-G_0-G_1 peak, DEVDase activities are still very low even 48 h after CPT treatment (Fig. 1*B*, *right*). Caspase inhibition in U-937 cells after CPT treatment abrogated completely the oligonucleosome-sized and high molecular weight DNA fragmentation for at least 8 h in U-937 cells (12). However, when cells appear in sub-G_0-G_1 peak, the presence of zVAD-fmk still completely abrogates the oligonucleosome-sized DNA fragmentation even 48 h after CPT treatment. In contrast, the presence of zVAD-fmk does not prevent the occurrence of high molecular weight DNA fragmentation 24 and 48 h after CPT treatment (Fig. 1*C*, *right*). Occurrence of high molecular weight DNA fragments was observed previously in necrotic cell death (25). To further investigate the effects of persistent caspase inhibition by zVAD-fmk on CPT-induced apoptosis, electron micrographs were analyzed. Fig. 2 shows that CPT induces within 4 h characteristic morphological changes associated with the apoptotic phenotype, including chromatin condensation and cell shrinkage in U-937 cells. In contrast, the presence of zVAD-fmk in CPT-treated cells inhibits completely the morphological events associated with apoptosis 4 h after drug treatment. However, cytolysis with microscopic features of necrosis including disruption of the plasma membrane, vacuolization, and scattered chromatin are observed 24 h after CPT treatment in the presence of zVAD-fmk (Fig. 2). These observations show that caspase inhibition shifts the death mechanism predominantly to necrosis, apoptosis being governed by a caspase activation event (26, 27).

Effect of zVAD-fmk on Expression and Activity of Cell Cycle-related Proteins in CPT-treated U-937 Cells. Induction of cell cycle arrest in response to DNA damage is a well-known phenomena. First, anticancer drugs including CPT can perturb the orderly progress of DNA replication fork and thus slow S phase and cell division. The inhibition of top 1 by CPT generates DNA double-strand breaks on collision of a replication fork with a top 1 cleavable complex. DNA elongation inhibition is one of the most explored processes to be implicated in the cytotoxic mechanism of action of top 1 inhibitors (1, 28). Inhibition of DNA synthesis is observed in CPT-treated cells in

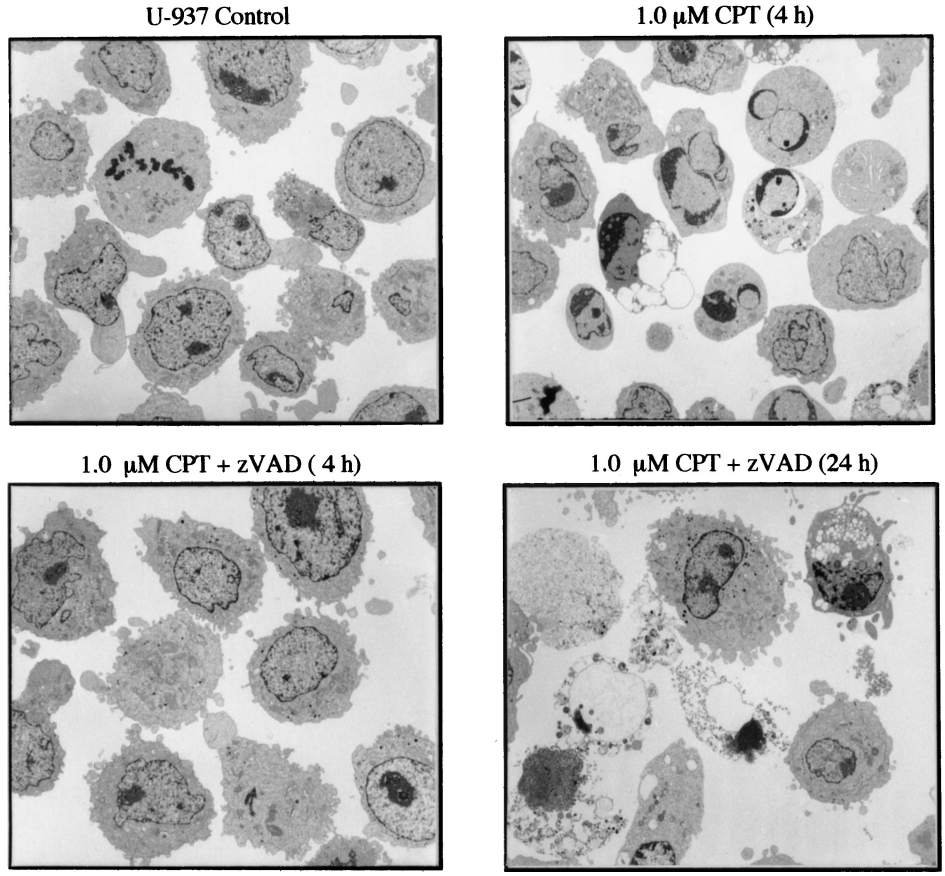

Fig. 2. The effects of caspase inhibition on cellular morphology in CPT-treated U-937 cells. Electron micrographs of control and CPT-treated U-937 cells in the absence or presence of zVAD-fmk. Cells were collected and processed for electron microscopy at the indicated times after drug treatment.

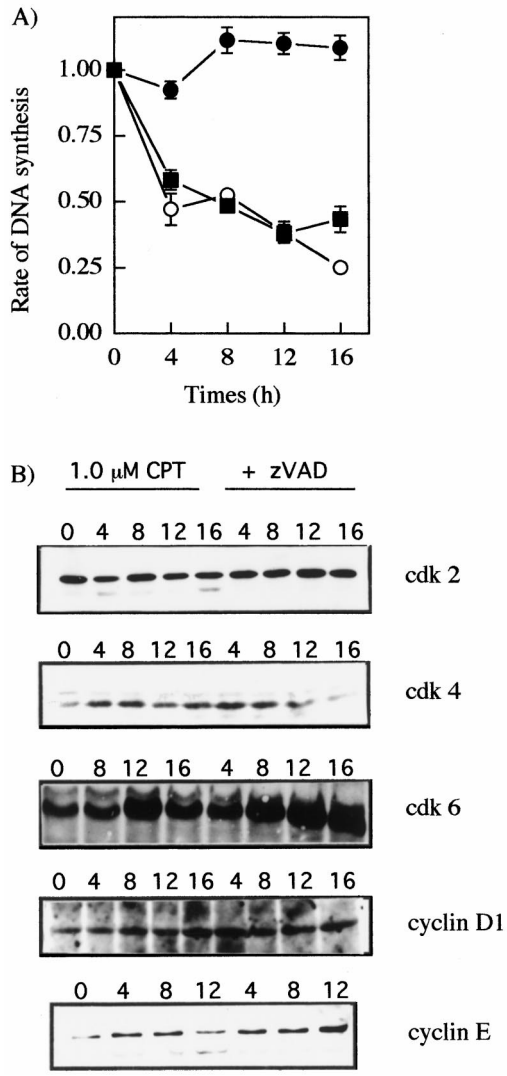

Fig. 3. The effects of zVAD-fmk on expression of cell cycle-related proteins in CPT-treated U-937 cells. *A*, kinetics of DNA synthesis after drug treatment in U-937 cells. At the indicated times (in h) after drug treatment (*x axis*), [^{3}H]thymidine incorporation was determined by 10-min pulse experiments. Values are expressed as the rate of DNA synthesis relative to control untreated cells. ○, CPT treatment; ●, zVAD-fmk treatment; ■, CPT + zVAD-fmk treatment. *Data points*, means of four independent determinations; *bars*, SE. *B*, kinetics of cdk and cyclin expression after CPT treatment in the absence or presence of zVAD-fmk. Whole-cell extracts were prepared as described under "Materials and Methods" from U-937 cells. cdk and cyclin proteins were detected using specific antibodies after SDS-PAGE and transfer to Immobilon-P membrane. *Numbers above lanes*, hours after drug treatment.

the presence or absence of zVAD-fmk (Fig. 3*A*). The persistent inhibition of DNA replication in cells in which caspases and apoptosis are inhibited could explain the observed slow passage through S-G_2, and it is consistent with the accumulation of these cells at the G_0-G_1 phase of the cell cycle. Anticancer drugs can also activate cell cycle checkpoints that are key cell cycle events that tightly control the transition of cells from one phase of the cell cycle to the next one. Expression of functional tumor suppressor gene *p53* participates actively in the G_1 checkpoint in response to DNA damage. However, several studies revealed that *p53* −/− cells can undergo through a G_1 checkpoint also. However, some cancer cells, including U-937 cells, lacking functional p53 because of gene deletion, mutation, or targeted disruption by the use of viral proteins show hypersensitivity to DNA damaging agents like CPT (9, 29–31). Thus, to further investigate the molecular determinants underlying the observed accumulation of CPT-treated cells at G_0-G_1 when caspase activities are inhibited, we monitored the expression and activity of the cell cycle components of the G_1 checkpoint. Expression study of the specific cdks and cyclins involved during G_1 phase and G_1-S transition of the cell cycle reveals no major changes in expression of cdk2, cdk4, cdk6, cyclin D1, and cyclin E in CPT-treated U-937 cells in the absence or presence of zVAD-fmk (Fig. 3*B*). Expression of cdk2 and cyclin E, the most important protein complex regulating G_1-S transition, remains unchanged whether cells rapidly undergo apoptosis (CPT alone) or accumulate in the G_0-G_1 phase of the cell cycle (CPT in the presence of zVAD-fmk). Whereas cyclin D1 expression remains stable, cdk4 expression falls and cdk6 expression increases in the presence of zVAD-fmk 16 h after CPT treatment. Such changes do not explain the accumulation of cells in the G_0-G_1 phase that occurs between 4 and 16 h after CPT treatment. Similarly, we detected no increased expression level of a variety of cdk inhibitors including p16, p21, p27, and p57 after CPT treatment in the presence of zVAD-fmk (data not shown). To validate these expression studies, kinetics of cdk2, cdk4, and cdk6 kinase activities were monitored from CPT-treated cells in the absence or presence of zVAD-fmk, where cells undergo apoptosis or accumulate in the G_0-G_1 phase of the cell cycle, respectively. As shown in Fig. 4, cotreatment of cells with or without zVAD-fmk did not significantly modulate the kinase activities of cdk2, cdk4, and cdk6 after CPT treatment. Mitotic catastrophe associated with aber-

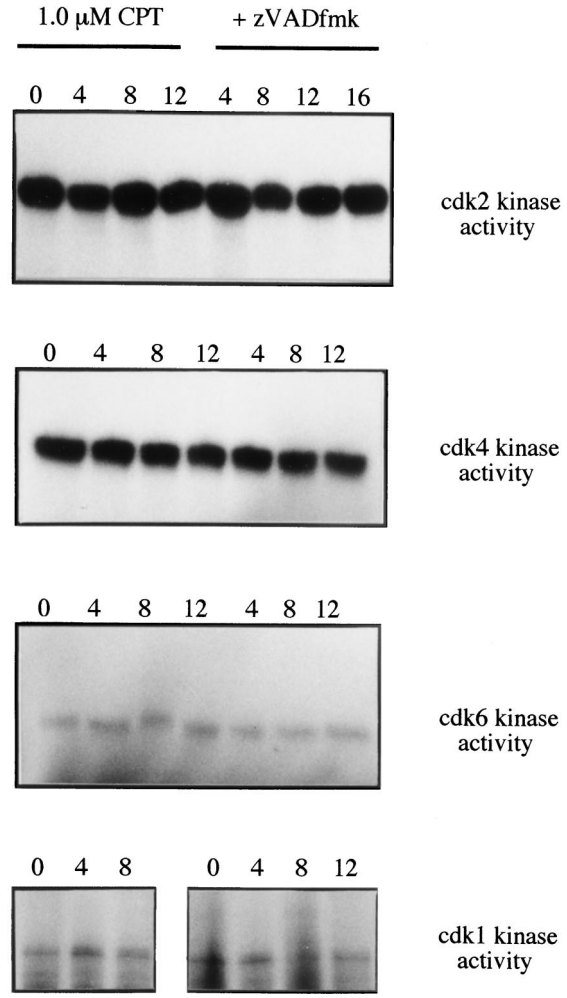

Fig. 4. Kinetics of cdk activities in CPT-treated U-937 cells in the absence or presence of zVAD-fmk. Immunocomplexes were obtained using specific antibodies and incubated in kinase buffer in the presence of [γ-^{32}P]ATP. The phosphorylated substrate was resolved by SDS-PAGE and visualized by autoradiography. *Numbers above lanes*, hours after drug treatment.

rant transient activation of cdc2/cdk1 has been suggested to contribute in apoptosis induced by several stimuli, including top 1 and top 2 inhibitors (32–35), whereas other studies have indicated that several agents including top 2 inhibitors induce apoptosis in a context of reduced expression of cdc2/cdk1 in temperature-sensitive mutants (36). In U-937 cells treated with CPT in either the presence or the absence of the caspase inhibitor zVAD-fmk, unscheduled activation or reduction in cdc2/cdk1 activity was not observed (Fig. 4).

Together, these results suggest that the observed accumulation of cells in G_0-G_1 does not implicate a classical driven G_1 checkpoint when caspase inhibition is enforced after CPT treatment. Moreover, slow passage through S-G_2 and accumulation of these cells at G_1 is associated more likely with the reported effects of CPT in: (*a*) mediating the inhibition of DNA elongation after stabilization of top 1-linked DNA strand breaks; and (*b*) preventing events into G_1 phase leading to replication complex initiation and stabilization involving top 1. Interaction of ongoing RNA transcription with top 1 cleavable complexes may also generate cytotoxic lesions that result in transient cell cycle arrest (1, 23, 28, 37). The importance of caspase activation during apoptosis has become eminently apparent in the last few years. However, enforced caspase inhibition after CPT treatment does not confer a survival advantage but shifts cells from apoptosis to massive necrotic cell death. Similar observations were reported previously in B lymphocytes treated with dexamethasone, where caspase inhibitors induced a switch from apoptosis to necrosis (27). Similarly, inducers of mitochondrial permeability transition have been shown to trigger caspase activation and apoptosis in thymocytes. Blocking caspase activities in these cells provoked a switch from apoptosis to necrosis (26). Finally, several studies have suggested that manipulation of cell cycle components can induce or inhibit apoptosis. However, no single cdk complex involved in the G_1 checkpoint has been associated with a common pathway of apoptosis (38). Our observations in this study do not suggest a positive or negative role for the cell cycle components of the G_1 checkpoint in apoptosis or necrosis. These results do not necessarily rule out the implication of these proteins in other instances of induced cell death.

Acknowledgments

We thank Myriam Beauchemin for technical assistance.

References

1. Gupta, M., Fujimori, A., and Pommier, Y. Eukaryotic DNA topoisomerase I. Biochim. Biophys. Acta, *1262:* 1–14, 1995.
2. Pommier, Y. DNA Topoisomerase II inhibitors. *In:* B. A. Teicher (ed.), Cancer Therapeutics: Experimental and Clinical Agents, pp. 153–174. Totowa, New Jersey: Humana Press Inc, 1997.
3. Kaufmann, S. H. Induction of endonucleolytic DNA cleavage in human acute myelogenous leukemia cells by etoposide, camptothecin, and other cytotoxic anticancer drugs: a cautionary note. Cancer Res., *49:* 5870–5878, 1989.
4. Barry, M. A., Behnke, C. A., and Eastman, A., Activation of programmed cell death (apoptosis) by cisplatin, other anticancer drugs, toxins and hyperthermia. Biochem. Pharmacol., *40:* 2353–2362, 1990.
5. Bertrand, R., Sarang, M., Jenkin, J., Kerrigan, D., and Pommier, Y. Differential induction of secondary DNA fragmentation by topoisomerase II inhibitors in human tumor cell lines with amplified c-*myc* expression. Cancer Res., *51:* 6280–6285, 1991.
6. Del Bino, G., and Darzynkiewicz, Z. Camptothecin, Teniposide, or 4′-(9-acridinylamino)-3-methanesulfon-m-anisidide, but not mitoxantrone or doxorubicin, induces degradation of nuclear DNA in the S-phase HL-60 cells. Cancer Res., *51:* 1165–1169, 1991.
7. Walker, P. R., Smith, C., Youdale, T., Leblanc, J., Whitfield, J. F., and Sikorska, M. Topoisomerase II-reactive chemotherapeutic drugs induce apoptosis in thymocytes. Cancer Res., *51:* 1078–1085, 1991.
8. Hickman, J. A. Apoptosis induced by anticancer drugs. Cancer Metastasis Rev., *11:* 121–139, 1992.
9. O'Connor, P. M., Jackman, J., Bae, I., Myers, T. G., Fan, S., Mutoh, M., Scudiero, D. A., Monks, A., Sausville, E. A., Weinstein, J. N., Friend, S., Fornace, A. J., and Kohn, K. W. Characterization of the *p53* tumor suppressor pathway in cell lines of the National Cancer Institute drug screen and correlations with the growth-inhibitory potency of 123 anticancer agents. Cancer Res., *57:* 4285–4300, 1997.
10. Dubrez, L., Savoy, I., Hamman, A., and Solary, E. Pivotal role of a DEVD-sensitive step in etoposide-induced and Fas-mediated apoptotic pathways. EMBO J., *15:* 5504–5512, 1996.
11. Martins, L. M., Kottke, T., Mesner, P. W., Basi, G. S., Sinha, S., Frigon, N., Tatar, E., Tung, J. S., Bryant, K., Takahashi, A., Svingen, P. A., Madden, B. J., McCormick, D. J., Earnshaw, W. C., and Kaufmann, S. H. Activation of multiple interleukin-1-β converting enzyme homologues in cytosol and nuclei of Hl-60 cells during etoposide-induced apoptosis. J. Biol. Chem., *272:* 7421–7430, 1997.
12. Sané, A. T., and Bertrand, R. Distinct steps in DNA fragmentation pathway during camptothecin-induced apoptosis involved caspase-, benzyloxycarbonyl- and *N*-tosyl-L-phenylalanylchloromethyl ketone-sensitive activities. Cancer Res., *58:* 3066–3072, 1998.
13. Alnemri, E. S. Mammalian cell death proteases: a family of highly conserved aspartate specific cysteine proteases. J. Cell Biochem., *64:* 33–42, 1997.
14. Cryns, V., and Yuan, J. Y. Proteases to die for. Genes Dev., *12:* 1551–1570, 1998.
15. Schmitt, E., Sane, A. T., and Bertrand, R. Activation and role of caspases in chemotherapy-induced apoptosis. Drug Resistance Updates, *2:* 21–29, 1999.
16. Kuida, K., Haydar, T. F., Kuan, C. Y., Gu, Y., Taya, C., Karasuyama, H., Su, M. S. S., Rakic, P., and Flavell, R. A. Reduced apoptosis and cytochrome c-mediated caspase activation in mice lacking caspase 9. Cell, *94:* 325–337, 1998.
17. Yoshida, H., Kong, Y. Y., Yoshida, R., Elia, A. J., Hakem, A., Hakem, R., Penninger, J. M., and Mak, T. W. Apaf1 is required for mitochondrial pathways of apoptosis and brain development. Cell, *94:* 739–750, 1998.
18. Liu, X. S., Zou, H., Slaughter, C., and Wang, X. D. DFF, a heterodimeric protein that functions downstream of caspase-3 to trigger DNA fragmentation during apoptosis. Cell, *89:* 175–184, 1997.
19. Enari, M., Sakahira, H., Yokoyama, H., Okawa, K., Iwamatsu, A., and Nagata, S. A caspase-activated DNAse that degrades DNA during apoptosis, and its inhibitor ICAD. Nature (Lond.), *391:* 43–50, 1998.
20. Halenbeck, R., Macdonald, H., Roulston, A., Chen, T. T., Conroy, L., and Wiiliams, L. T. CPAN, a human nuclease regulated by the caspase-sensitive inhibitor DFF45. Curr. Biol., *8:* 537–540, 1998.
21. Kerr, J. F., Wyllie, A. H., and Currie, A. R. Apoptosis. a basic biological phenomenon with wide-ranging implications in tissue kinetics. Br. J. Cancer, *26:* 239–257, 1972.
22. Schmitt, E., Cimoli, G., Steyeart, A., and Bertrand, R. Bcl-x_L modulates apoptosis induced by anticancer drugs and delays DEVDase and DNA fragmentation-promoting activities. Exp. Cell Res., *240:* 107–121, 1998.
23. Bertrand, R., O'Connor, P., Kerrigan, D., and Pommier, Y. Sequential administration of camptothecin and etoposide circumvents the antagonistic cytotoxicity of simultaneous drug administration in slowly growing human carcinoma, HT-29 cells. Eur. J. Cancer, *28A:* 743–748, 1992.
24. Thornberry, N. A., Ranon, T. A., Pieterson, E. P., Rasper, D. M., Timkey, T., Garciacalvo, M., Houtzager, V. M., Nordstrom, P. A., Roy, S., Vaillancourt, J. P., Chapman, K. T., and Nicholson, D. W. A combinatorial approach defines specificities of members of the caspase family and granzyme B: functional relationships established for key mediators of apoptosis. J. Biol. Chem., *272:* 17907–17911, 1997.
25. Bicknell, G. R., and Cohen, G. M. Cleavage of DNA to large kilobase pair fragments occurs in some forms of necrosis as well as apoptosis. Biochem. Biophys. Res. Comm., *207:* 40–47, 1995.
26. Hirsch, T., Marchetti, P., Susin, S. A., Dallaporta, B., Zamzami, N., Marzo, I., Geuskens, M., and Kroemer, G. The apoptosis-necrosis paradox: apoptogenic proteases activated after mitochondrial permeability transition determine the mode of cell death. Oncogene, *15:* 1573–1581, 1997.
27. Lemaire, C., Andreau, K., Souvannavong, V., and Adam, A. Inhibition of caspase activity induces a switch from apoptosis to necrosis. FEBS Lett., *425:* 266–270, 1998.
28. Kaufmann, S. H. Cell death induced by topoisomerase-targeted drugs—more questions than answers. Biochim. Biophys. Acta, *1400:* 195–211, 1998.
29. Thomas, A., Elrouby, S., Reed, J. C., Krajewski, S., Silber, R., Potmesil, M., and Newcomb, E. W. Drug-induced apoptosis in B-cell chronic lymphocytic leukemia: relationship between *p53* gene mutation and Bcl-2/Bax proteins in drug resistance. Oncogene, *12:* 1055–1062, 1996.
30. Waldman, T., Lengauer, C., Kinzler, K. W., and Vogelstein, B. Uncoupling of S phase and mitosis induced by anticancer agents in cells lacking p21. Nature (Lond.), *381:* 713–716, 1996.
31. Gupta, M., Fan, S. J., Zhan, Q. M., Kohn, K. W., O'Connor, P. M., and Pommier, Y. Inactivation of p53 increases the cytotoxicity of camptothecin in human colon HCT116 and breast MCF-7 cancer cells. Clin. Cancer Res., *3:* 1653–1660, 1997.
32. Shi, L., Nishioka, W. K., Th'ng, J., Bradbury, E. M., Litchfield, D. W., and Greenberg, A. H. Premature p34cdc2 activation required for apoptosis. Science (Washington DC), *263:* 1143–1145, 1994.
33. Pandey, S., and Wang, E. Cells en route to apoptosis are characterized by the upregulation of c-fos, c-myc, c-jun, cdc2, and RB phosphorylation, resembling events of early cell-cycle traverse. J. Cell. Biochem., *58:* 135–150, 1995.
34. Shimizu, T., O'Connor, P. M., Kohn, K. W., and Pommier, Y. Unscheduled activation of cyclin B1/Cdc2 kinase in human promyelocytic leukemia cell line HL60 cells undergoing apoptosis induced by DNA damage. Cancer Res., *55:* 228–231, 1995.
35. Yao, S. L., McKenna, K. A., Sharkis, S. J., and Bedi, A. Requirement of $p34^{cdc2}$ kinase for apoptosis mediated by the Fas/Apo-1 receptor and interleukin 1-β-converting enzyme-related proteases. Cancer Res., *56:* 4551–4555, 1996.
36. Martin, S. J., McGahon, A. J., Nishioka, W. K., LaFace, D., Guo, X., Th'ng, J., Bradbury, E. M., and Green, D. R. p34cdc2 and apoptosis. Science (Washington DC), *269:* 106–107, 1995.
37. O'Connor, P. M., Nieves-Neira, W., Kerrigan, D., Bertrand, R., Goldman, J., Kohn, K. W., and Pommier, Y., S-phase population analysis does not correlate with the cytotoxicity of camptothecin and 10,11-methylenedioxycamptothecin in human colon carcinoma HT-29 cells. Cancer Commun., *3:* 233–240, 1991.
38. Kasten, M. M., and Giordano, A. pRB and the CDKs in apoptosis and the cell cycle. Cell Death Differ., *5:* 132–140, 1998.